Published in final edited form as:
*Biochem J*. 2012 January 1; 441(1): 379–386. doi:10.1042/BJ20111050.

# A Common Single Nucleotide Polymorphism A118g of the Mu Opioid Receptor Alters Its N-glycosylation and Protein Stability

**Peng Huang**[1], **Chongguang Chen**[1], **Stephen D Mague**[2,#], **Julie A Blendy**[2,3], and **Lee-Yuan Liu-Chen**[1,*]

[1]Department of Pharmacology, Temple University School of Medicine, Philadelphia, PA19140

[2]Department of Pharmacology, University of Pennsylvania Perelman School of Medicine, Philadelphia, PA 19104

[3]Abramson Cancer Center, University of Pennsylvania Perelman School of Medicine, Philadelphia, PA 19104

## Synopsis

The A118G single nucleotide polymorphism (SNP) of the human mu opioid receptor (hMOPR) gene OPRM1 results in an amino acid substitution (N40D). Subjects homozygous for G118 allele were reported to require higher morphine doses to achieve adequate analgesia and G118 allele was more prevalent among drug abusers. However, changes in the MOPR protein associated with this SNP are unknown. Using a knock-in mouse model (G/G mice) that possesses the equivalent nucleotide/amino acid substitution (N38D; A112G) of the A118G in the hMOPR gene , we investigated N-linked glycosylation status of thalamic and striatal MOPR in G/G mice vs A/A (wildtype) mice. The relative molecular mass ($M_r$) of MOPR determined with immunoblotting was lower in G/G mice than in A/A mice. Following treatment with PNGase F, which removes all N-linked glycans, both MOPR variants had identical $M_r$, indicating that this discrepancy was due to a lower level of N-glycosylation of the MOPR in G/G mice. In CHO cells stably expressing hMOPRs, G118/D40-hMOPR had lower $M_r$ than A118/N40-hMOPR, which was similarly due to differential N-glycosylation. Pulse-chase studies revealed that the half-life of the mature form of G118/D40-hMOPR (∼12h) was shorter than that of A118/N40-hMOPR (∼28h). Thus, A118G SNP reduces MOPR N-glycosylation and protein stability.

### Keywords

mu opioid receptor; A118G; glycosylation; N-glycan; G protein-coupled receptor; protein stability

## Introduction

MOPRs, belonging to the seven transmembrane receptor (7TMR) family or G protein-coupled receptor (GPCR) family, mediate pharmacological effects of morphine and other μ-preferring compounds. Activation of the MOPRs produces analgesia, reward, mood changes, sedation, respiratory depression, immuno-suppression, decreased gastrointestinal motility, increased locomotor activity, tolerance and dependence [for reviews, see [1,2]]. Bergen *et al.* [3] and Bond *et al.* [4] first reported the existence of A118G SNP in the coding region in the exon 1 of the hMOPR gene (OPRM1). This SNP has been found to have the

*Address correspondence to: Dr. Lee-Yuan Liu-Chen, Department of Pharmacology, Temple University School of Medicine, 3420 North Broad Street, Philadelphia, PA 19140, USA Tel: 1-215-707-4188; Fax: 1-215-707-7068; lliuche@temple.edu.
#Current address: Department of Psychology and Neuroscience, Duke University, Genome Sciences Research Building II, 572 Research Drive, Room 3021, Durham, NC 27710.

highest overall allelic frequency of all the OPRM1 coding region variants. The G118 allele frequency varies widely across populations: 1% to 3% in African Americans, 10-14% in both Caucasians and Hispanics, 35-49% in Asians and 8-21% in other populations [reviewed in [5]]. Four clinical studies conducted on East Asians showed that subjects homozygous for G118 needed higher morphine doses to attain adequate pain control following surgery than those of homozygous for A118 [6-9]. In addition, subjects of G/G or A/G genotype have better treatment outcomes for nicotine and alcohol abuse [10-12] and higher propensity for drug addiction [13-16][reviewed in [17]].

To delineate the mechanisms underlying the changes associated with the OPRM1 A118G SNP in humans, Mague *et al.* [18] generated a knock-in mouse line that possesses the mouse equivalent of the A118G variant in the hMOPR gene (Oprm1 A112G). Mice homozygous for the G112 allele (G/G mice) had lower antinociceptive responses to morphine than mice homozygous for the A112 allele (A/A mice) [18], indicating that these mice represent good animal models for studying the A118G SNP of the MOPR in humans. In addition, G/G mice showed greatly attenuated morphine-induced hyperactivity, and impaired development of locomotor sensitization [18]. Moreover, female, but not male, G/G mice exhibited reductions in the rewarding properties of morphine and the aversive components of naloxoneprecipitated morphine withdrawal [18]. More recently, Ramchandani *et al.*[19] established two mouse lines with humanized mouse MOPR genes (h/mMOPR), where the mouse Oprm1 exon 1 was replaced by the corresponding human sequence and carried the A118 or G118 allele. Using brain microdialysis, they found a 4-fold greater peak dopamine response to an alcohol challenge in G118-h/mMOPR than in A118-h/mMOPR mice [19]. This is consistent with the results of their human studies that alcohol induced a striatal dopamine release only in carriers of the minor G118 allele [19].

N-linked glycosylation is a common post-translational modification of 7TMRs. The A118G SNP changes Asn to Asp at position 40 (N40D) in the N-terminal domain and removes one of the five potential N-linked glycosylation sites of hMOPR (Fig. 1). Although the consensus sequence of N-glycosylation sites is a tripeptide motif of -Asn-X-Thr/Ser-, not all such motifs are glycosylated in a glycoprotein [20]. One possible explanation is that the primary, secondary, and/or tertiary structures of the peptide around the consensus N-glycosylation sites play roles in substrate recognition by the enzymes (e.g., oligosaccharyl transferase) [21]. Thus, it is not clear whether the loss of an - Asn-X-Thr/Ser- motif due to A118G SNP, leads to changes in N-glycosylation of the MOPR, and if so, whether this SNP impacts on stability of the MOPR protein as it is well-documented that glycans augment overall stability of glycoproteins [reviewed in [22]], including several 7TMRs [23-25].

Similar to the human SNP, the A112G variant in the mouse alters Asn to Asp at position 38 (N38D) of the mouse MOPR [18], eliminating a potential N-linked glycosylation site accordingly (Fig. 1). We have observed significant reductions of MOPR protein levels in the thalamus and whole brain of G/G mice, compared with A/A mice [18]. In the present studies, we investigated whether the SNP affected N-glycosylation of MOPR by comparing the G112/D38-MOPR in G/G mice with A112/N38-MOPR in A/A mice using immunoblotting combined with deglycosylation experiments. Similar experiments were conducted on the two hMOPR variants (A118/N40-hMOPR and G118/D40-hMOPR) stably expressed in CHO cells. In addition, pulse-chase experiments were performed with those cell lines to determine the half-lives of A118/N40-hMOPR and G118/D40-hMOPR.

# Experimental

## Materials

The reagents were obtained from indicated suppliers: wheat germ lectin (WGL)-Sepharose 6MB from Amersham Pharmacia (Uppsala, Sweden); [$^{35}$S]L-methionine/[$^{35}$S]L-cysteine (1175.0 Ci/mmol) from PerkinElmer Life Sciences; Dulbecco's modified Eagle's medium without L-methionine and L-cysteine from Invitrogen (Carlsbad, CA); Triton X-100 from Sigma-Aldrich (St. Louis, MO); Geneticin from Mediatech (Herndon, VA); Hind III and other restriction enzymes from Promega (Madison, WI); Immobilon-P PVDF transfer membrane from Millipore Corporation (Billerica, MA); Mini Complete™ Protease Inhibitor Cocktail was from Roche (Nutley, NJ); HA.11, a product of Covance (Cumberland, VA); PNGase F and relevant buffers from New England Biolabs (Ipswich, MA); 0.2-μm spin cartridges from Rainin Co., (Emeryville, CA); SuperSignal West Pico Chemiluminescent Substrate Solutions from Pierce Co. (Rockford, IL). Reagent-grade chemicals were purchased from Sigma-Aldrich (St. Louis, MO) or Fisher (Pittsburgh, PA).

***Anti-mu C*** is a rabbit polyclonal anti-MOR antibody generated as described in our previous reports [26,27] against the sequence CT$^{383}$NHQLENLEAETAPLP$^{398}$ (the mu C peptide), which corresponds to the last 16 amino acids (383-398) of the C-terminal domain predicted from the cloned rat MOPR (GenBank: NM_013071) and which is identical among human, rat and mouse. The antiserum was generated in rabbits and purified by use of the mu C peptide affinity chromatography,

***Animals:*** **A112G-MOPR knock-in mice (A/A and G/G mice)** were generated on a C57BL/6 genetic background in Dr. Blendy's laboratory [18]. **MOPR-knockout (-/-) mice** were originally developed in the lab of Dr. John Pintar (University of Medicine and Dentistry of New Jersey) by disruption of exon-1 of the MOPR-1 gene through homologous recombination [28]. The MOPR knockout (-/-) mice used in this study were derived following at least 10 generations of successive backcrossing of 129S6×C57BL/6J heterozygotes to C57BL/6J mice.

## Brain membrane preparation

Brains from MOPR(-/-) mice or A/A112 and G/G112 littermate mice were collected. The striatum or thalamus tissues were dissected and homogenized in 8 volumes of 25 mM Tris-HCl buffer/pH 7.4 containing 1 mM EDTA and 0.1mM PMSF (pH 7.4) on ice and then centrifuged at 100,000 *g* for 30 min. Pellets were twice rinsed with 25 mM Tris-HCl buffer and resuspended in 0.32 M sucrose in 50 mM Tris-HCl/pH 7.0. Suspended membranes were passed through a 26.5 G needle 5 times and then frozen at - 80°C until use.

## Solubilization and WGL affinity purification of MOPRs

Thalamic membranes from 5 male and 5 female A/A or G/G mice were combined. Membrane proteins (2-3 mg) were solubilized in 0.8 ml TTSEC buffer (50 mM Tris-HCl/ pH7.4, 2% Triton X-100, 150 mM NaCl, 5 mM EDTA and Roche tablet of protease inhibitors at 1 pill per 10 ml) with 1mM PMSF at 4°C for 3 h. Supernatants were collected after centrifugation at 100,000 *g* for 30 min and mixed with 50 μl of wheat germ lectin (WGL) Sepharose 6MB at 4°C for 1 h. The beads were washed with cold TTSEC with 0.2% Triton X-100 for three times. The WGL beads-associated proteins were dissociated/eluted in 30 μl 10 × denaturation solution [5% SDS, 0.4M dithiothrietol (DTT)] by incubation for 10 min at 37°C.

### Treatment of WGL eluate with PNGase F

The experiments were performed according to our published procedure [29]. To 3 μl of the dissociated protein complex described above, 3 μl each of 10 × G7 Reaction Buffer (0.5 M sodium phosphate/pH 7.5) and 10% NP-40 was added, followed by 21 μl of water. The 30-μl reaction mix was incubated at 37°C overnight in the absence or presence of 1 μl of PNGase F. An equal volume (30 μl) of 2 × Laemmli sample buffer was added to the reaction mix. The 60-μl sample was incubated at 37°C for 10 min and loaded onto SDS-PAGE for separation.

**Immunoblotting of MOPRs in mouse brains and 3HA-tagged hMOPRs in CHO cells** was carried out according to our published method [27,30]. Protein samples were prepared with 2 × Laemmli sample buffer and loaded (20 μg protein per lane) for SDS-PAGE and Western blot was performed with anti-mu C or an antibody against the HA-tag (HA.11), followed by goat anti-rabbit or anti-mouse IgG conjugated with HRP (1:5,000), respectively, and then reacted with enhanced chemiluminescence (ECL) Western blotting detection reagents. Images were captured with a FujiFilm LAS-1000 Imaging System.

**Oligodeoxynucleotide-directed mutagenesis** was carried out as described previously [31] on the hMOPR cDNA with the overlap polymerase chain reaction method. The A118/N40- or G118/D40-hMOPR cDNA (*NcoI*/*XbaI*), tagged with 3HA (*Hind III*/*NcoI*) 5′ to the initiation codon, was subcloned into *Hin*dIII and *Xba*I sites of the mammalian expression vector pcDNA3. The cDNA sequences were determined to confirm the presence of desired mutations and the absence of unwanted mutations.

### Stable Expression of the A118/N40-hMOPR or G118/D40-hMOPR in CHO Cells

Transfection of CHO cells with the cDNA clones was performed with Lipofectamine according to the manufacturer's instructions, and cells were grown under the selection pressure of Geneticin (1 mg/ml). Mixed CHO cell clones expressing 3HA-A118/N40-hMOPR or 3HA-G118/D40-hMOPR were established as described previously [31].

**Pulse-chase experiments** were performed as described previously [32].

**Metabolic Labeling with $^{35}$S-Labeled l-Methionine/l-Cysteine—**CHO cells stably expressing 3HA tagged A118/N40- or G118/D40-hMOPR were washed with and preincubated in Dulbecco's modified Eagle's medium without l-methionine and l-cysteine for 1 h at 37°C. Pulse was performed in the fresh Met/Cys-free medium containing 150 μCi/ml of [$^{35}$S]l-methionine/[$^{35}$S]l-cysteine (1175.0 Ci/mmol). After 30-min incubation at 37°C, pulse was terminated by washing cells once with the chase medium (OPTI-MEM supplemented with 10% fetal bovine serum and 5 mM l-methionine), and chase was performed for indicated time periods.

**Immunoprecipitation of $^{35}$S-Labeled G118/D40- or A118/N40-hMOPR—**At each chase time point, medium was aspirated and cells in two wells of 6-well plates were briefly washed and detached with 10 mM phosphate buffer/1 mM EDTA/1 mM glucose. Two wells of labeled cells were then collected in 1.5 ml microfuge tubes, pelleted by centrifugation at 1,000 *g*, and stored at -80°C until further experiments. Cells were solubilized with 400 μl of TTSEC buffer, end-to-end mixed for 30 min at 4°C, and centrifuged at 13,500 *g* for 10 min. Supernatants were filtered through 0.2-μm spin cartridges. Immunoprecipitation was performed twice in tandem with HA antibody (HA.11) followed by PANSORBIN and centrifugation to purify the $^{35}$S-labeled receptor for satisfactory signal/noise.

**SDS-PAGE and Imaging—**An 8% SDS-PAGE with Tricine buffer system was used to separate proteins. Completed gels were dried on a Bio-Rad gel dryer. The gels were then exposed to a storage phosphor screen for 5 days, and the autoradiograms were acquired using a Cyclone PhosphorImager (PerkinElmer Life Sciences). The intensities of radioactive bands were analyzed with the OptiQuant program (PerkinElmer Life Sciences), with local background subtracted from each lane.

**Curve fitting—**Transformation of the immature receptor form (precursors) to the mature form and turnover of both receptor forms appear to follow the first-order kinetics. All analyses were performed using Prism 3.0 to fit the data to the equations [33]:

$$Y = A(e^{-k_e t} - e^{-k_a t}) \quad (\text{for mature form})$$
$$Y = Ae^{-k_e t} \quad (\text{for precursors})$$

where $Y$ is the amount of MOPR, $A$ is a constant for each equation, $k_a$ is the transformation rate constant of the immature to mature receptor, $k_e$ is the turnover rate constant of the mature or immature receptor, and $t$ is the time of the chase. The turnover rate constant ($k_e$) means the fraction of the receptor degraded per unit of time. Half-life ($t_{1/2}$) is the time for the receptor to reduce by 50%, and it is equal to $0.693/k_e$.

## Results

### The relative molecular mass ($M_r$) of MOPR in G/G mice was lower than that in A/A mice, which is due to differences in N-glycosylation of MOPR

Immunoblotting of the MOPR was performed on membranes of the thalamus and striatum of female mice. In the thalami of A/A or G/G mice, anti-mu C labeled several bands, one of which was absent in the MOPR(-/-) mice, indicating that this diffuse protein band represents the MOPR. Notably, the $M_r$ range of the MOPR in A/A mice was higher than that in G/G mice: 56–67 kDa (median, 62 kDa) in the A/A mice (Fig. 2, left panel, lane 1 vs lane 3) and 51-62 kDa (median, 55 kDa) in G/G mice (Fig. 2, left panel, lane 2 vs lane 3). Again using the MOPR(-/-) mouse tissue as the negative control, we found that in the striata of A/A mice, the MOPR band labeled by anti-mu C was more diffuse [27], with a $M_r$ range of 58–82 kDa (median, 72 kDa) (Fig. 2, right panel, lane 1 vs lane 3). Similarly, the striatal MOPR band in G/G mice had a lower $M_r$ range, 53-76 kDa (median, 66 kDa) (Fig. 2, right panel, lane 2 vs lane 3). The same experiments were performed on brain tissues of male mice and similar results were obtained (data not shown). There were no sex differences in the $M_r$ of the MOPR.

We then tested the hypothesis that the differences in the $M_r$'s of the MOPRs in A/A and G/G are due to varying extents of glycosylation from the loss of one glyclosylation site (N38) in the G/G mice. To this end, we enriched MOPRs by wheat germ lectin (WGL) affinity chromatography [29] and treated the MOPRs with PNGase F, which removes all N-linked glycans. Thalamic membranes of A/A or G/G mice (half males and half females) were pooled and solubilized with 2% Triton X-100 and incubated with WGL Sepharose 6MB beads and eluted with 5% SDS, which enriched the MOPR approximately 30-fold. Western blotting of WGL affinity-purified materials with anti-mu C showed that the thalamic MOPRs in A/A and G/G mice migrated as a single diffuse band with a median $M_r$ of 62 kDa and 55 kDa (Fig. 3, lanes 1 and 2), respectively. Treatment of the WGL affinity-purified materials with PNGase F resulted in an increase in the mobility of thalamic MOPRs in both A/A and G/G mice on SDS–PAGE (Fig. 3, lanes 3 and 4), compared with the untreated controls (Fig. 3, lanes 1 and 2). More importantly, the diffuse MOPR bands with different

median $M_r$'s in the two mouse lines (Fig. 3, lanes 1 and 2) became sharp bands with a lower and identical $M_r$ (41 kDa) (Fig. 3, lanes 3 and 4). Thus, the difference in $M_r$'s of the MOPRs in A/A and G/G mice is due to differential N-linked glycosylation.

### The $M_r$ of G118/D40-hMOPR was lower than that of A118/N40-hMOPR, due to different N-glycosylation, when both were stably expressed in cultured cells

N-linked glycosylation in 7TMRs has been shown to play important role in proper folding and trafficking of the receptor proteins [for example, [23]]. We thus investigated if the SNP affects stability and trafficking of the MOPR. Since it is not feasible to carry out such studies in brain tissues, we used cells in culture. Cell lines (CHO cells and HEK293 cells) stably expressing 3HA-tagged A118/N40-hMOPR and G118/D40-hMOPR were established. Immunoblotting of CHO cell membranes with anti-HA revealed that both A118/N40-hMOPR and G118/D40-hMOPR migrated as broad and diffuse bands and the G118/D40-hMOPR exhibited a lower median $M_r$ (76 kDa) (Fig. 4, lane 3) than A118/N40-hMOPR (81 kDa) (Fig. 4, lane 2). Similarly, in HEK293 cells both MOPR variants migrated as diffuse bands and G118/D40-hMOPR had a lower median $M_r$ (80 kDa) (Fig. 4, lane 5) than A118/N40-hMOPR (85 kDa) (Fig. 4, lane 4).

CHO cells stably expressing A118/N40-hMOPR or G118/D40-hMOPR were solubilized with Triton X-100, and hMOPRs enriched using WGL Sepharose 6MB affinity purification. Immunoblotting with anti-HA revealed A118/N40-hMOPR and G118/D40-hMOPR as two diffuse bands with median $M_r$'s of 81 and 76 kDa, respectively (Fig. 5, lanes 1 and 2). Following removal of N-glycans by treatment with PNGase F, the difference in the $M_r$'s of A118/N40-hMOPR and G118/D40-hMOPR disappeared, and either hMOPR was recognized as a diffuse band with identical median $M_r$ of 48 kDa (Fig. 5, lanes 3 and 4). These results indicate that the differences in the $M_r$'s of the two MOPR variants are due to varying degrees of N-linked glycosylation.

### The half-life of G118/D40-hMOPR was shorter than that of A118/N40-hMOPR expressed in CHO cells

We then examined if the A118G SNP affected maturation and stability of the MOPR with pulse-chase experiments on hMOPRs stably expressed in CHO cells (Fig. 6). Cells were incubated with [$^{35}$S]Met/Cys-containing medium at 37°C for 60 min (pulse). Following removal of the medium, cells were incubated with complete medium (chase) for specified time periods indicated in Fig. 6. At 0 h, the Mr ranges of the precursors of A118/N40-hMOPR and G118/D40-hMOPR were 52-56 kDa and 50-54 kDa, respectively. The precursors were gradually transformed into the mature/fully glycosylated forms of the 81 kDa-band and 76 kDa-band, respectively over time (0-2h). The two MOPR variants have similar extents of conversion from the precursor form to the mature form (from 0 h to 2 h, 87±25 vs 82±16 %, n=3). The peak levels of the mature forms were reached at 2 h for both hMOPR variants (Fig. 6A). With their peak levels as 100%, the levels of the mature forms of A118/N40-hMOPR and G118/D40-hMOPR were quantified at various time points (Fig. 6B) and their half-lives were determined. As evident in Fig. 6B, the fully glycosylated G118/D40-hMOPR was degraded faster than the A118/N40-hMOPR counterparts with half-lives of 11.6±1.9 h (n=3) and 27.7±5.5 h (n=3), respectively ($p<0.05$) (Table 1). The levels of the precursors of A118/N40-hMOPR and G118/D40-hMOPR were also quantified (Fig. 6B). With their initial levels at 0 h as 100%, the precursors of the two MOPR variants had similar half-lives (1.3±0.2 vs 1.2±0.2 h, n=3) (Table 1).

## Discussion

The current studies provided the first experimental evidence that A118G SNP reduced the N-linked glycosylation of the MOPR and, more importantly, the reduction in N-linked glycosylation resulted from this SNP compromised stability of the MOPR protein.

### Decreased $M_r$ of MOPR by A118G/A112G is indicative of its reduced N-glycosylation

We found by immunoblotting that G112/D38-MOPR (G/G mice) had lower $M_r$ than A112/N38-MOPR (A/A mice) in the thalamus, which is consistent with our previous report [18]. In addition, we demonstrated a similar difference in $M_r$ of the MOPRs in the striatum (Fig. 2). In addition, in stable cell lines G118/D40-hMOPR had lower $M_r$ than A118/N40-hMOPR (Fig. 4). The findings that following deglycosylation with PNGase F, both variants of the hMOPR or the mouse MOPR had the same Mr (Fig. 3 and Fig. 5) support the notion that the decreases in $M_r$ of the MOPR by the A118G or A112G SNP are due to varied N-glycosylation status, which may imply the elimination of one of the N-linked glycans by the SNP. It has been demonstrated that, in general, glycoproteins from the human brain show similar profiles of brain region-specific N-glycans as those from mouse and rat brains [34]. Therefore, what we observed on the MOPRs in the mouse brains is likely to reflect those in the human brain.

### Reduced N-glycosylation of MOPR by A118G mutation results in its lower protein stability in CHO cells

It is generally accepted that N-glycans are important to the overall stability of glycoproteins [reviewed in [22]]. Our observations that the mature/fully glycosylated A118/N40-hMOPR had a longer half-life than those of G118/D40-hMOPR are consistent with this notion. These results are in accord with the findings on several 7TMRs, including the human kappa opioid receptor [23], vasopressin 1a receptor [24] and protease-activated receptor-2 [25]. For example, mutation of the two *N*-linked glycosylation sites of hKOPR (hKOPR-N25/39Q) led to faster degradation of the mature mutant receptor and thereby decreased receptor expression. One notable difference is that the effects observed with A118G in the hMOPR are due to elimination of only one of the five consensus glycosylation sites, whereas those found for other 7TMRs resulted from total elimination of N-linked glycosylation.

### Is the A118G/A112G-induced lower protein stability of MOPR related to the lower protein level?

The mature forms of the G118/D40-hMOPR stably expressed in CHO cells had a shorter half-life than those of the A118/N40-hMOPR (Fig. 6), but their precursors had similar half-lives and turnover rates, suggesting that the G118/D40-hMOPR may have lower expression levels. However, the impact of A118G/A112G on MOPR level is not uniform and our results obtained in CHO cells appears to be applicable to brain regions or cell lines that showed decreased MOPR levels, but no those that did not. *In vivo*, A112G knock-in mice (G/G mice) has lower MOPR protein level in the thalamus and in the whole brain than wildtype mice (A/A mice) [18]. In contrast, in the striatum and hippocampus, G/G mice and A/A mice had similar levels of MOPR (manuscript in preparation). In addition, in the humanized G118-h/mMOPR and A118-h/mMOPR mice, no genotype differences in MOPR densities were observed in the striatum and the ventral tegmental area [19]. Moreover, in the human carriers of the G118 allele, the number of [$^3$H]DAMGO binding sites was unaffected in the secondary somatosensory area and the ventral posterior part of the lateral thalamic tissue, compared with the homozygous A118 carriers [35]. It is noteworthy, however, that in this study 86% of the human carriers of the G118 allele were heterozygotes [35]. Recently smokers heterozygous for the G118 allele have been shown to have lower levels of MOPR binding potential as measured by $^{11}$C-carfentanil in certain unilateral or bilateral brain

regions, such as the amygdala, thalamus, and anterior cingulate cortex, compared to those homozygous for the A118 allele. In contrast, no differences were observed in other areas including the ventral striatum/nucleus accumbens and caudate [36]. *In vitro*, A118G mutation of the hMOPR decreased receptor expression in stably transfected HEK293 [37,38] and AV-12 cells [38] or transiently transfected CHO cells [39], as revealed by [$^3$H]DAMGO binding and/or immunoblotting, but did not change protein expression of the hMOPR in transiently transfected COS [40], HEK293 and AV-12 cells [38]. Thus, the A118G/A112G SNP either decreases or does not change expression of MOPR in different brain regions or cell lines. The variations in the impact of the SNP on the MOPR expression in different cell lines and brain regions may be due to differences in glycosylation machinery. The MOPR has been shown to have brain region-specific N-glycosylation patterns [27], which is confirmed in this studies (Fig. 2, thalamus vs striatum) and is likely the result of differential expression of various enzymes involved in glycosylation across brain regions. Indeed, Matsuhashi *et al.*[41] observed region-specific expression of glycotransferases in adult mouse brain. It is noteworthy that no RNA editing of the MOPR occurs in either the striatum or thalamus [27]. Nevertheless, it remains unknown whether the varied N-glycosylation patterns of the MOPR in the two brain areas resulted from the brain region-specific glycosylation of Asn residues and/or different N-glycan compositions attached to the Asn residues. Thus, a likely explanation for our observation is that the A118G/A112G mutation leads to brain area-specific changes in N-glycan contents and thereby differentially affects protein expression of MOPR across brain regions. Similarly, the median Mr's of the A118/N40-hMOPR and the G118/D40-hMOPR are higher in HEK 293 cells than in CHO cells (Fig. 4), suggesting higher levels of glycosylation in HEK293 cells. However, how the extents and types of glycosylation affect glycoprotein expression are not well understood.

Similarly, A1 18G/A112G decreased or did not change MOPR mRNA levels depending on brain regions. In humans, A118G lowers levels of MOPR mRNA in the cortical lobes and pons [39]. Decreased MOPR mRNA was also found in G/G mice, compared with A/A mice, in the periaqueductal gray, hypothalamus, ventral tegmental area, nucleus accumbens and cortex [18], while no difference was found in the hippocampus [18] and thalamus (our unpublished data). Although MOPR protein levels in most of these brain regions have not been compared between wildtype and the A118G (A112G) variants, it is clear that lower protein expression of the MOPR is not due to lower mRNA level since in the thalamus of G/G mice, the protein level of the MOPR is lower, but its mRNA is unchanged, compared with that of A/A mice.

## Reduced N-glycosylation of MOPR by A118G SNP has little effect on binding affinities of opioid ligands

Regarding the binding affinities of exogenous ligands, including DAMGO, morphine, morphine-6-glucuronide, CTOP, diprenorphine and/or naloxone, there were no differences observed between G118/D40- and A118/N40-hMOPR expressed in cell lines such as AV-2 [4,38], COS [40] and HEK293 [37] cells, or between G112/D38-MOPR and A112/N38-MOPR in G/G and A/A mice, respectively [18]. Although G118/D40-hMOPR expressed in AV-12 cells was initially reported to have three times higher binding affinity of β-endorphin, an endogenous ligand, than A118/N40-hMOPR [4], this finding was not reproduced in two studies using COS [40] and HEK293 [37] cells. Furthermore, MOPRs in the brains of G/G and A/A mice [18] or G118-h/mMOPR and A118-h/mMOPR expressed in CHO cells [19] did not differ in their binding affinity for β-endorphin. In addition, G118/D40- and A118/N40-hMOPR expressed in COS cells had similar binding affinities for other endogenous opioids, including met-enkephalin and dynorphin A [40]. Therefore, A118G SNP alters N-glycosylation of the MOPR in the N-terminal domain without changing its ligand binding

affinities. This is not unexpected as the ligand binding pocket of the MOPR has been proposed to be formed mainly by amino acids in its transmembrane domains and, to much lower extents, extracellular domains [42,43].

### Detection of endogenous MOPR in brain by western blot

Our experience demonstrates that it is difficult to identify endogenous MOPR by immunoblotting, in part due to its low abundance *in vivo* and heavy and heterogeneous glycosylation, which results in a broad and diffuse band and reduced band intensity [see [26] for review]. Using tissues from MOPR(-/-) mice as the negative control is particularly useful for identification of the receptor since antibodies, even after purification, recognize other non-specific protein bands [18,27]. In the literature, the MOPR bands detected by immunological methods following SDS-PAGE can be divided into two categories: broad and diffuse ones with higher relative molecular masses ($M_r$'s) vs. sharp ones with lower $M_r$'s [For examples, see [44] and [45]]. Researchers including our group have taken multiple approaches to demonstrate the MOPR mainly as a diffuse band by covalent labeling with [$^3$H]beta-funaltrexamine ([$^3$H]beta-FNA)] [29,46], receptor phosphorylation [47-49] and immunoblotting with anti-MOPR antibodies [18,27,30]. The rigor and convergence of pharmacological and biochemical data provide confidence in the unequivocal identification of MOPR [see [26] for review]. This single broad band of the mature MOPR has a $M_r$ range between 58 to 97 kDa and the median $M_r$ above 54 kDa, depending on cell lines, brain regions and species. Upon deglycosylation to remove N-linked glycans, MOPRs became sharp bands with $M_r$'s close to the theoretical molecular mass (∼43 kDa) of the deduced amino acid sequences [see [26] for review].

Our concerns about the reliability of the anti-MOPR antibodies, several of which are commercially available, are not unique. A number of reports from different groups suggest that even with good choices of peptide epitopes as antigens, it is fortuitous if one obtains good antibodies for immunoblotting and/or immunohistochemisty of 7TMRs/GPCRs. In addition, receptor antibodies should be validated carefully with multiple techniques, such as knock-out animals, other than using blocking peptides solely [see [50] for review].

## Conclusion

Using a genetic mouse model and cultured cell lines, the common A118G SNP in the human MOPR gene has been shown to reduce the N-glycosylation and protein stability of the MOPR, which may account for the reduction of MOPR expression in certain brain regions. These findings may shed lights on the molecular mechanisms of the decreased clinical opioid potency in G118 allele carriers.

## Acknowledgments

This study is supported by NIH grants DA027066, DA17302 and P30 DA13429.

## Reference list

1. Kieffer BL. Trends Pharmacol Sci. 1999; 20:19–26. [PubMed: 10101958]
2. Gaveriaux-Ruff C, Kieffer BL. Neuropeptides. 2002; 36:62–71. [PubMed: 12359497]
3. Bergen AW, Kokoszka J, Peterson R, Long JC, Virkkunen M, Linnoila M, Goldman D. Mol Psychiatry. 1997; 2:490–494. [PubMed: 9399694]
4. Bond C, LaForge KS, Tian M, Melia D, Zhang S, Borg L, Gong J, Schluger J, Strong JA, Leal SM, Tischfield JA, Kreek MJ, Yu L. Proc Natl Acad Sci USA. 1998; 95:9608–9613. [PubMed: 9689128]

5. Kreek MJ, Bart G, Lilly C, LaForge KS, Nielsen DA. Pharmacol Rev. 2005; 57:1–26. [PubMed: 15734726]
6. Chou WY, Yang LC, Lu HF, Ko JY, Wang CH, Lin SH, Lee TH, Concejero A, Hsu CJ. Acta Anaesthesiol Scand. 2006; 50:787–792. [PubMed: 16879459]
7. Chou WY, Wang CH, Liu PH, Liu CC, Tseng CC, Jawan B. Anesthesiology. 2006; 105:334–337. [PubMed: 16871067]
8. Sia AT, Lim Y, Lim EC, Goh RW, Law HY, Landau R, Teo YY, Tan EC. Anesthesiology. 2008; 109:520–526. [PubMed: 18719451]
9. Hayashida M, Nagashima M, Satoh Y, Katoh R, Tagami M, Ide S, Kasai S, Nishizawa D, Ogai Y, Hasegawa J, Komatsu H, Sora I, Fukuda K, Koga H, Hanaoka K, Ikeda K. Pharmacogenomics. 2008; 9:1605–1616. [PubMed: 19018716]
10. Oslin DW, Berrettini W, Kranzler HR, Pettinati H, Gelernter J, Volpicelli JR, O'Brien CP. Neuropsychopharmacology. 2003; 28:1546–1552. [PubMed: 12813472]
11. Kim SG, Kim CM, Choi SW, Jae YM, Lee HG, Son BK, Kim JG, Choi YS, Kim HO, Kim SY, Oslin DW. Psychopharmacology (Berl). 2009; 201:611–618. [PubMed: 18795264]
12. Lerman C, Wileyto EP, Patterson F, Rukstalis M, Audrain-McGovern J, Restine S, Shields PG, Kaufmann V, Redden D, Benowitz N, Berrettini WH. Pharmacogenomics J. 2004; 4:184–192. [PubMed: 15007373]
13. Szeto CY, Tang NL, Lee DT, Stadlin A. Neuroreport. 2001; 12:1103–1106. [PubMed: 11338173]
14. Bart G, Heilig M, LaForge KS, Pollak L, Leal SM, Ott J, Kreek MJ. Mol Psychiatry. 2004; 9:547–549. [PubMed: 15037869]
15. Bart G, Kreek MJ, Ott J, LaForge KS, Proudnikov D, Pollak L, Heilig M. Neuropsychopharmacology. 2005; 30:417–422. [PubMed: 15525999]
16. Nishizawa D, Han W, Hasegawa J, Ishida T, Numata Y, Sato T, Kawai A, Ikeda K. Neuropsychobiology. 2006; 53:137–141. [PubMed: 16679777]
17. Mague SD, Blendy JA. Drug Alcohol Depend. 2010; 108:172–182. [PubMed: 20074870]
18. Mague SD, Isiegas C, Huang P, Liu-Chen LY, Lerman C, Blendy JA. Proc Natl Acad Sci USA. 2009; 106:10847–10852. [PubMed: 19528658]
19. Ramchandani VA, Umhau J, Pavon FJ, Ruiz-Velasco V, Margas W, Sun H, Damadzic R, Eskay R, Schoor M, Thorsell A, Schwandt ML, Sommer WH, George DT, Parsons LH, Herscovitch P, Hommer D, Heilig M. Mol Psychiatry. In Press.
20. Petrescu AJ, Milac AL, Petrescu SM, Dwek RA, Wormald MR. Glycobiology. 2004; 14:103–114. [PubMed: 14514716]
21. Petrescu AJ, Milac AL, Petrescu SM, Dwek RA, Wormald MR. Glycobiology. 2004; 14:103–114. [PubMed: 14514716]
22. Sola RJ, Griebenow K. J Pharm Sci. 2009; 98:1223–1245. [PubMed: 18661536]
23. Li JG, Chen C, Liu-Chen LY. Biochem. 2007; 46:10960–10970. [PubMed: 17711303]
24. Hawtin SR, Davies AR, Matthews G, Wheatley M. Biochem J. 2001; 357:73–81. [PubMed: 11415438]
25. Compton SJ, Sandhu S, Wijesuriya SJ, Hollenberg MD. Biochem J. 2002; 368:495–505. [PubMed: 12171601]
26. Huang P, Liu-Chen LY. Front Biosci (Elite Ed). 2009; 1:220–227. [PubMed: 19482639]
27. Huang P, Chen C, Xu W, Yoon SI, Unterwald EM, Pintar JE, Wang Y, Chong PL, Liu-Chen LY. Biochem Biophys Res Commun. 2008; 365:82–88. [PubMed: 17980152]
28. Schuller AG, King MA, Zhang J, Bolan E, Pan YX, Morgan DJ, Chang A, Czick ME, Unterwald EM, Pasternak GW, Pintar JE. Nat Neurosci. 1999; 2:151–156. [PubMed: 10195199]
29. Liu-Chen LY, Chen C, Phillips CA. Mol Pharmacol. 1993; 44:749–756. [PubMed: 8232225]
30. Huang P, Xu W, Yoon SI, Chen C, Chong PL, Unterwald EM, Liu-Chen LY. Brain Res. 2007; 1184:46–56. [PubMed: 17980352]
31. Huang P, Li J, Chen C, Visiers I, Weinstein H, Liu-Chen LY. Biochem. 2001; 40:13501–13509. [PubMed: 11695897]

32. Chen C, Li JG, Chen Y, Huang P, Wang Y, Liu-Chen LY. J Biol Chem. 2006; 281:7983–7993. [PubMed: 16431922]
33. Tallarida, RJ.; Murray, RB. Manual of Pharmacologic Calculations with Computer Programs. Springer-Verlag; New York: 1987.
34. Albach C, Klein RA, Schmitz B. Biol Chem. 2001; 382:187–194. [PubMed: 11308017]
35. Oertel BG, Kettner M, Scholich K, Renne C, Roskam B, Geisslinger G, Schmidt PH, Lotsch J. J Biol Chem. 2009; 284:6530–6535. [PubMed: 19116204]
36. Ray R, Ruparel K, Newberg A, Wileyto EP, Loughead JW, Divgi C, Blendy JA, Logan J, Zubieta JK, Lerman C. Proc Natl Acad Sci USA. 2011; 108:9268–9273. [PubMed: 21576462]
37. Beyer A, Koch T, Schroder H, Schulz S, Hollt V. J Neurochem. 2004; 89:553–560. [PubMed: 15086512]
38. Kroslak T, LaForge KS, Gianotti RJ, Ho A, Nielsen DA, Kreek MJ. J Neurochem. 2007; 103:77–87. [PubMed: 17877633]
39. Zhang Y, Wang D, Johnson AD, Papp AC, Sadee W. J Biol Chem. 2005; 280:32618–32624. [PubMed: 16046395]
40. Befort K, Filliol D, Decaillot FM, Gaveriaux-Ruff C, Hoehe MR, Kieffer BL. J Biol Chem. 2001; 276:3130–3137. [PubMed: 11067846]
41. Matsuhashi H, Horii Y, Kato K. J Neurochem. 2003; 84:53–66. [PubMed: 12485401]
42. Strahs D, Weinstein H. Protein Eng. 1997; 10:1019–1038. [PubMed: 9464566]
43. Xu W, Li J, Chen C, Huang P, Weinstein H, Javitch JA, Shi L, de Riel JK, Liu-Chen LY. Biochem. 2001; 40:8018–8029. [PubMed: 11434771]
44. Xu Y, Gu Y, Xu GY, Wu P, Li GW, Huang LY. Proc Natl Acad Sci USA. 2003; 100:6204–6209. [PubMed: 12719538]
45. Garzon J, Juarros JL, Castro MA, Sanchez-Blazquez P. Mol Pharmacol. 1995; 47:738–744. [PubMed: 7723734]
46. Chen C, Xue JC, Zhu J, Chen YW, Kunapuli S, de Riel JK, Yu L, Liu-Chen LY. J Biol Chem. 1995; 270:17866–17870. [PubMed: 7629089]
47. Deng HB, Yu Y, Wang H, Guang W, Wang JB. Brain Res. 2001; 898:204–214. [PubMed: 11306006]
48. Yu YK, Zhang L, Yin XX, Sun H, Uhl GR, Wang JB. J Biol Chem. 1997; 272:28869–28874. [PubMed: 9360954]
49. Carman CV, Barak LS, Chen C, Liu-Chen LY, Onorato JJ, Kennedy SP, Caron MG, Benovic JL. J Biol Chem. 2000; 275:10443–10452. [PubMed: 10744734]
50. Michel MC, Wieland T, Tsujimoto G. Naunyn Schmiedebergs Arch Pharmacol. 2009; 379:385–388. [PubMed: 19172248]


## Abbreviations

| | |
|---|---|
| **7TMR** | seven transmembrane receptor |
| **A/A mice** | mice homogenous for MOPR A112 allele |
| **Asn/N** | asparagine |
| **Asp/D** | aspartic acid |
| **DAMGO** | ([D-Ala$^2$, N-MePhe$^4$, Gly-ol]-enkephalin |
| **ECL** | enhanced chemiluminescence |
| **G/G mice** | mice homogenous for MOPR G112 allele |
| **GPCR** | G protein-coupled receptor |
| **hKOPR** | human kappa opioid receptor |
| **hMOPR** | human mu opioid receptor |

| | |
|---|---|
| **h/mMOPR** | humanized mouse MOPR, where the mouse Oprm1 exon 1 was replaced by the corresponding human sequence |
| **SNP** | single nucleotide polymorphism |
| **WGL** | wheat germ lectin |


**Figure 1. The amino acid sequences of the N-terminal domains of human and mouse MOPRs**

Potential N-linked glycosylation sites are in red. The common amino acids are highlighted in yellow. The conservative substitutions are shaded in grey.

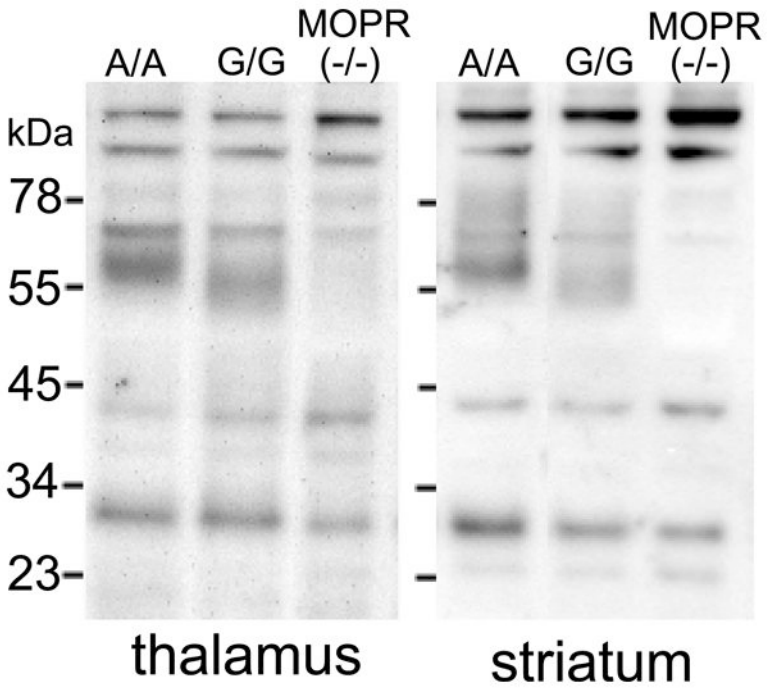


**Figure 2. Immunoblotting of the MOPRs in the thalami and striata of A/A mice, G/G mice and MOPR(-/-) mice**

Brain membranes were prepared from thalami or striata of adult female mice. Membrane proteins were resolved with 8% SDS–PAGE and immunoblotted with anti-mu C (1:5000), an affinity-purified polyclonal anti-MOR antibody we generated, as described in Materials and Methods. Each figure is a representative of the three independent experiments performed with tissues from different cohorts of female mice. Male mice yielded similar results (not shown).

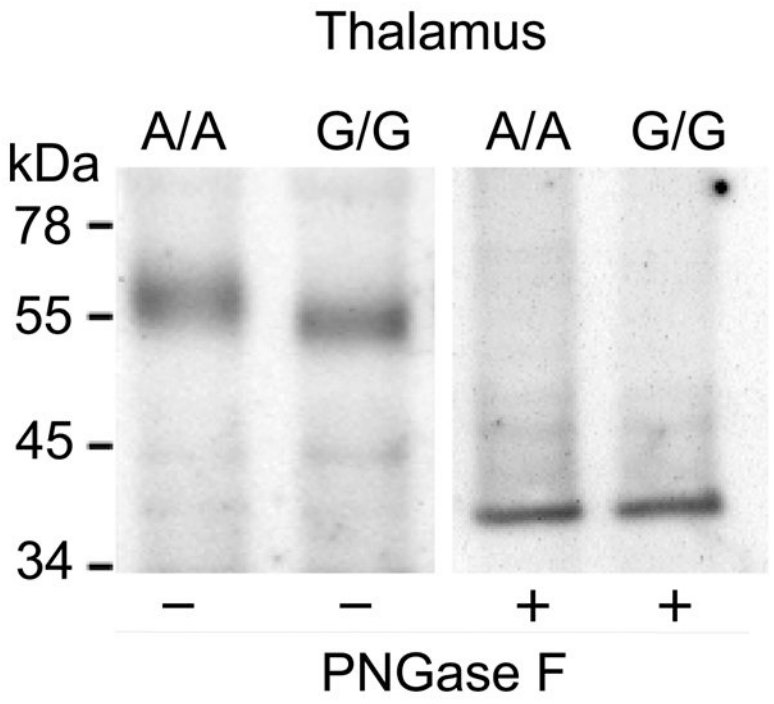


**Figure 3. Deglycosylation with PNGase F of MOPRs from thalami of A/A and G/G mice**

Thalamic membranes of A/A or G/G mice (mixed gender: 50% of each sex) were pooled and solubilized with 2% Triton X-100. The solubilized preparations were incubated with the wheat germ lectin (WGL) Sepharose 6MB beads and the bound glycoproteins were eluted with 2 × Laemmli sample buffer. The amount of eluate was adjusted to have similar MOPR levels. The eluate was left untreated or treated with PNGase F, resolved with 8% SDS–PAGE, and immunoblotted with anti-mu C (1:5000) as described in Fig.1. This figure is from one of the two independent experiments performed with similar results.

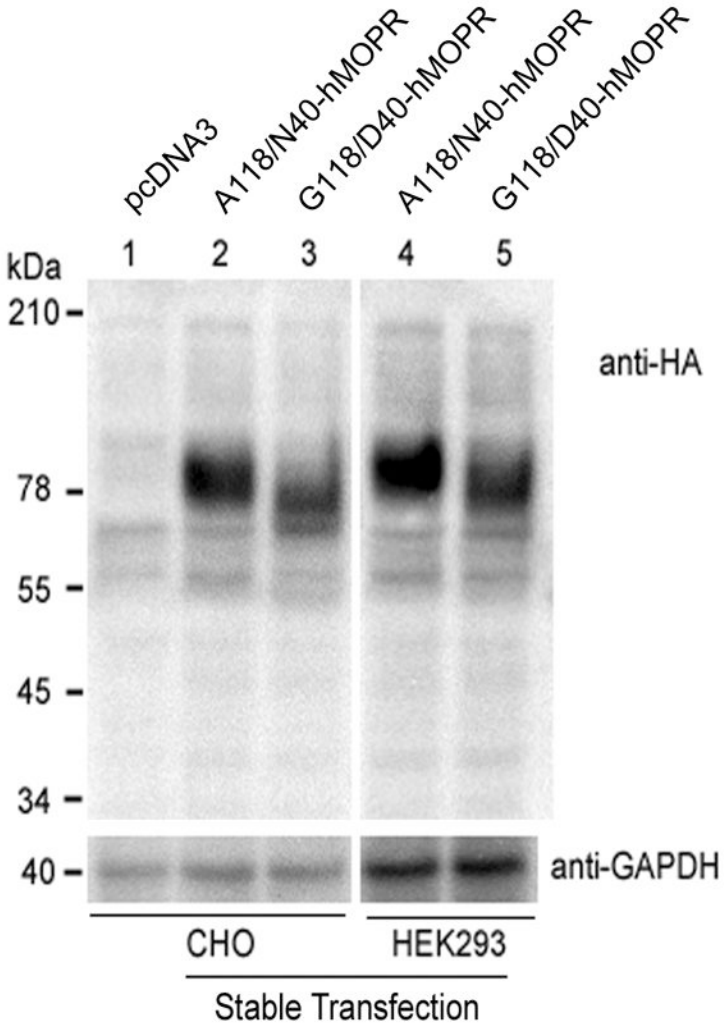


**Figure 4. Immunoblotting of the wild-type and A118G mutant of hMOPR (A118/N40-hMOPR and G118/D40-hMOPR, respectively) stably expressed in CHO and HEK293 cells**

CHO cells were stably transfected with 3HA tagged A118/N40- or G118/D40-hMOPR cDNA in the mammalian expression vector pcDNA3. Cells from stable mixed clones were collected and the protein contents resolved with 8% SDS–PAGE and immunoblotted with monoclonal anti-HA antibody HA.11. After stripping, the same blot was then processed for immunoblotting with mouse anti-GAPDH-HRP-conjugated. Each figure is from one of two independent experiments performed with similar results.

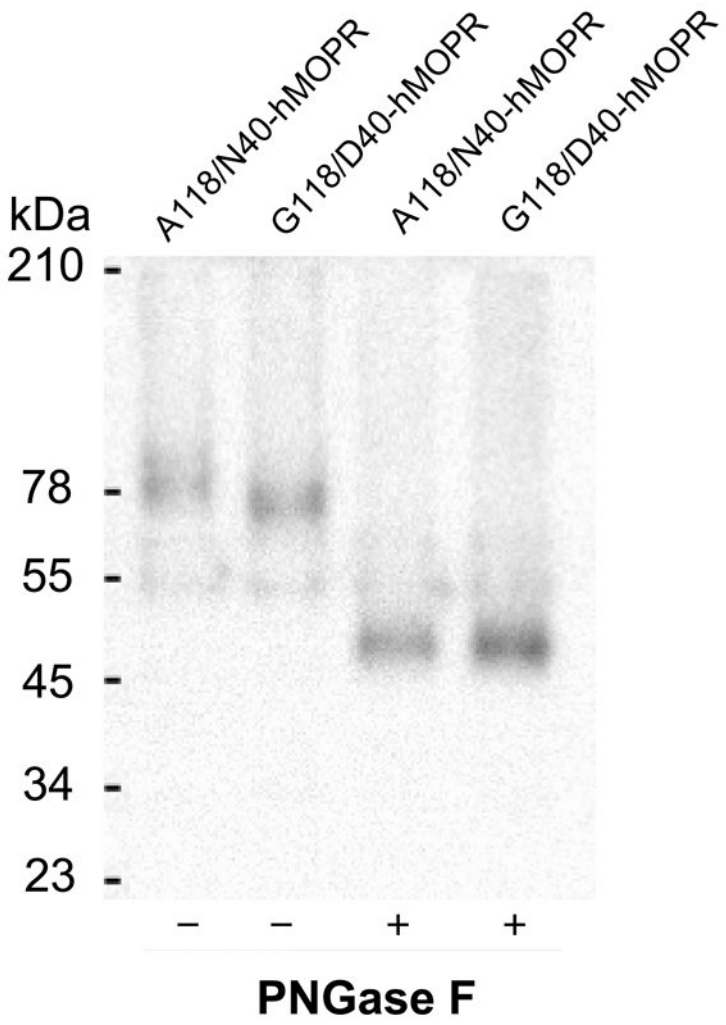


**Figure 5. Deglycosylation with PNGase F of the wild-type and A118G mutant of hMOPR (A118/N40-hMOPR and G118/N40-hMOPR, respectively) stably expressed in CHO cells**

Cells were solubilized with 2% Triton X-100. The A118/N40- or G118/D40-hMOPR was partially purified by WGL affinity chromatography, left untreated or treated with PNGase F and resolved with 8% SDS–PAGE as described in the Fig. 3 legend, and immunoblotted with HA.11 described in the Fig.4 legend. The amount of eluate was adjusted to have similar MOPR levels. Each figure shown is from one of three independent experiments with similar results.

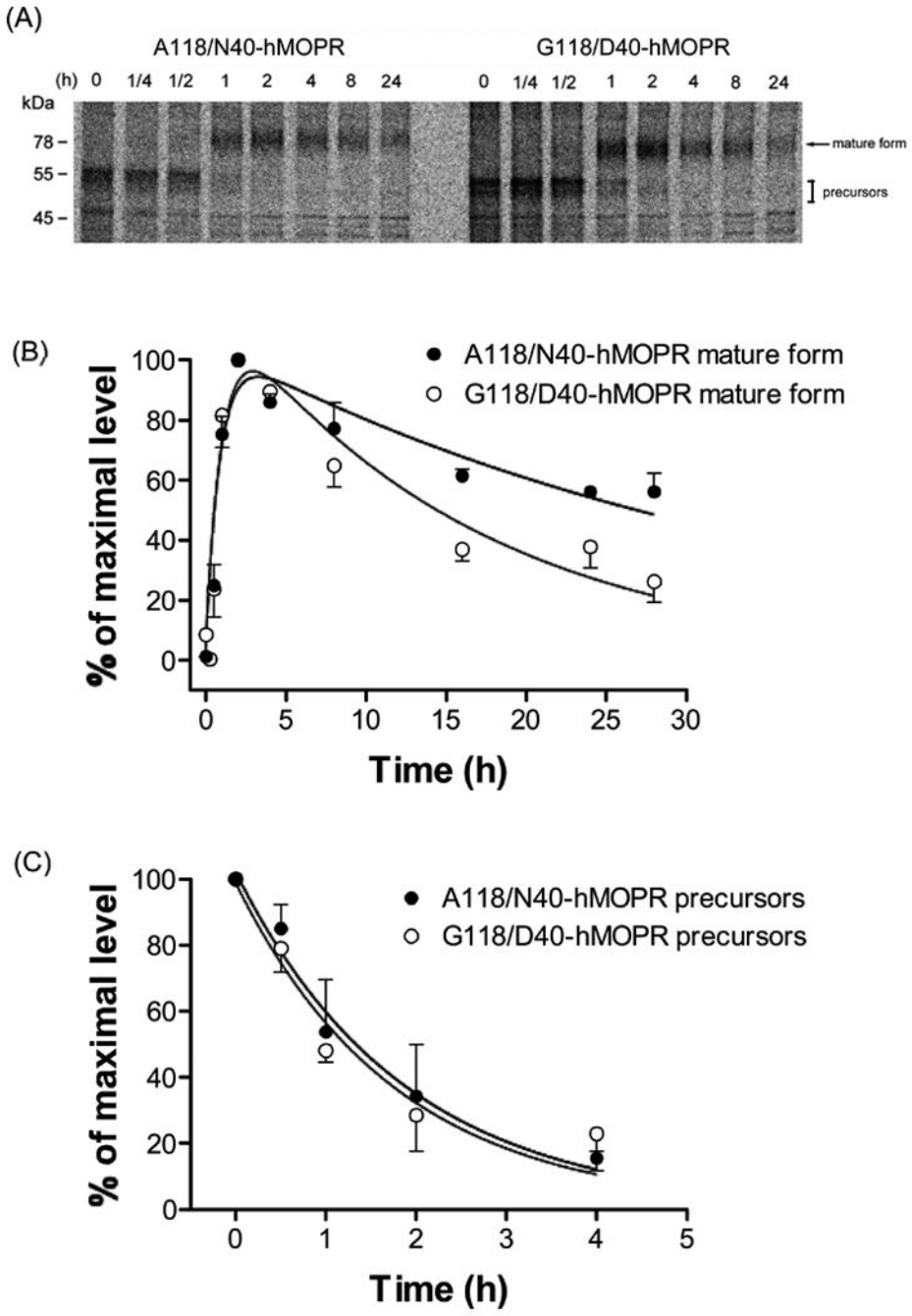


**Figure 6. Pulse-chase experiments of wildtype and A118G mutant of hMOPR (A118/N40-hMOPR and G118/D40-hMOPR, respectively) stably expressed in CHO cells**

Cells were metabolically labeled with [$^{35}$S]Met/Cys at 37°C for 60 min (pulse). Medium was aspirated, and cells were incubated with complete medium (chase) for specified time periods. Cells were solubilized and immunoprecipitated with HA.11 antibody twice in tandem. Immunoprecipitated materials were resolved with SDS-PAGE and gels were dried. The gels were then exposed to a storage phosphor screen for 5 days, and the autoradiograms were acquired. (A) shows a representative autoradiogram. The intensities of [$^{35}$S]-labeled protein bands were analyzed and quantified for the mature forms (B) and the precursors (C) as described in Methods. The signals for mature forms and precursors were normalized

against their maximal signals observed at time points 2h and 0h, respectively. The experiment was performed three times with similar results. Each value in (B) and (C) is mean ± s.e.m. (n=3).

## Table 1

Half-lives ($t_{1/2}$) of both the mature and precursor forms of A118/N40-hMOPR and G118/D40-hMOPR.

| | $t_{1/2}$ (h) | |
|---|---|---|
| | **mature forms** | **precursors** |
| A118/N40-hMOPR | 27.7 ± 5.0 | 1.3 ± 0.2 |
| G118/D40-hMOPR | 11.6 ± 1.9 * | 1.2 ± 0.2 |

Values of $t_{1/2}$ were determined from the data in Fig.6 as described in experimental procedures (see “Pulse-chase experiments/Curve fitting”). The data shown in the table are the mean ± SEM of three independent experiments.

* $P < 0.05$, compared to the A118/N40-hMOPR group using two-tailed Student's *t*-test.